



Published in final edited form as:

Organometallics. 2009 ; 28(5): 1350–1357. doi:10.1021/om800986s.

Dipolar Second-Order Nonlinear Optical Chromophores Containing Ferrocene, Octamethylferrocene, and Ruthenocene Donors and Strong π -Acceptors: Crystal Structures and Comparison of π -Donor Strengths

Tiffany L. Kinnibrugh[†], Seyhan Salman[§], Yulia A. Getmanenko[§], Veaceslav Coropceanu[§], William W. Porter III[‡], Tatiana V. Timofeeva[†], Adam J. Matzger[‡], Jean-Luc Brédas[§], Seth R. Marder[§], and Stephen Barlow^{§,*}

Department of Natural Sciences, New Mexico Highlands University, Las Vegas, NM 87701; School of Chemistry and Biochemistry and Center for Organic Photonics and Electronics, Georgia Institute of Technology, Atlanta, GA 30332-0400; Department of Chemistry, University of Michigan, Ann Arbor, MI 48109-1055

Abstract

Crystal structures have been determined for six dipolar polyene chromophores with metallocenyl – ferrocenyl (Fc), octamethylferrocenyl (Fc^m), or ruthenocenyl (Rc) – donors and strong heterocyclic acceptors based on 1,3-diethyl-2-thiobarbituric acid or 3-dicyanomethylidene-2,3-dihydrobenzothiophene-1,1-dioxide. In each case, crystals were found to belong to centrosymmetric space groups. For one example, polymer-induced heteronucleation revealed the existence of two additional polymorphs, which were inactive in second-harmonic generation, suggesting that they were also centrosymmetric. The bond-length alternations between the formally double and single bonds of the polyene bridges are reduced compared to simple polyenes, indicating significant contribution from charge-separated resonance structures, although the metallocenes are not significantly distorted towards the $[(\eta^6\text{-fulvene})(\eta^5\text{-cyclopentadienyl})\text{metal(II)}]^+$ extreme. DFT geometries are in excellent agreement with those determined crystallographically; while the π -donor strengths of the three metallocenyl groups are insufficiently different to result in detectable differences in the crystallographic bond-length alternations, the DFT geometries, as well as DFT-calculations of partial charges for atoms, suggest that π -donor strength decreases in the order Fc^m >> Fc > Rc. NMR, IR and electrochemical evidence also suggests that octamethylferrocenyl is the stronger π -donor, exhibiting similar π -donor strength to a *p*-(dialkylamino)phenyl group, while ferrocenyl and ruthenocenyl show very similar π -donor strengths to one another in chromophores of this type.

Email: stephen.barlow@chemistry.gatech.edu.

[†]NMHU

[§]Georgia Tech

[‡]Univ. Michigan

Supporting Information Available: X-ray data (CIF format). Table of selected crystal and refinement parameters; figures showing atom numbering schemes for structures of **1–6**; details of PIHn studies of **3**; discussion of crystal packing for **1–6**; list of NMR chemical shifts and assignments for **1–6** and **IX**; and complete calculated charge-density data (PDF format). This material is available free of charge via the Internet at <http://pubs.acs.org>.

Introduction

Group 8 metallocenes are among the most extensively investigated organometallic donors in donor- π -acceptor second-order NLO chromophores.¹ A few studies have involved ruthenocenyl, Rc, or extensively methylated ferrocenyl donors such as 2,3,4,5,1',2',3',4'-octamethylferrocenyl, Fc'', or nonamethylferrocenyl, Fc*; however, most have employed the unsubstituted ferrocenyl group, Fc.² Ionization potentials for the relevant parent metallocenes indicate that the *electron-transfer donor* strength of these metallocenyl units, i.e. the strength of these species as donors in electron-transfer reactions or electron-transfer-type optical transitions, decreases in the order Fc'' (or Fc*) > Fc > Rc.^{3,4} For chromophores with a given π -bridging group and acceptor, the energies of the lowest-energy vis-NIR transitions follow the trend Fc'' < Fc < Rc, consistent with assignment of this band as a metal-to-acceptor charge transfer.⁵ However, the relative π -donor strengths of these different metallocenyl units are less straightforward to assess. The π -donor strength can be thought of as the ability to couple to an attached π -system and can be gauged to the extent to which zwitterionic resonance structures of the type shown in Figure 1a contribute to the ground-state structure. Insight into the importance of the zwitterionic resonance form may potentially be gained from crystal structures of metallocenyl-polyene-acceptor chromophores with strong π -acceptor groups. Increased π -donation from donor to acceptor should be manifested in a decrease of the bond-length alternation between formally double and single CH—CH bonds in the polyene bridge, by bond-length changes in the acceptor group, and by geometric changes in the metallocenyl group. In the case of metallocenyl donors and where the acceptor is a directly attached carbocation, contributions can be anticipated from the $[(\eta^6\text{-fulvene})(\eta^5\text{-cyclopentadienyl})\text{metal(II)}]^+$ limiting structure, with the $[(\eta^1\text{-alkyl})\text{bis}(\eta^5\text{-cyclopentadienyl})\text{metal(IV)}]^+$ limiting structure also being a possible contributor (Figure 1b, ii and iii, respectively). In the case of cationic systems where ferrocenyl and ruthenocenyl groups compete to stabilize a full positive charge – the $[\text{Fc}(\text{CH})\text{Rc}]^+$ ion,⁶ related species derived from mixed-metal metallocenophanes,^{6,7} and the $[\text{Fc}(\text{CH})_3\text{Rc}]^+$ ion⁸ – crystallographic data indicate the presence of “normal” ferrocenes and $[(\eta^6\text{-fulvene})\text{CpRu}]^+$ groups suggesting that, at least in these types of systems, ruthenocenyl acts as a stronger π -donor than ferrocenyl. In the crystal structure of $[\text{Fc}''(\text{CH})_3\text{Fc}]^+[\text{BF}_4]^-$ both metallocenyl groups are somewhat distorted towards an $[(\eta^6\text{-fulvene})\text{CpM}]^+$, but with the metallocenyl distortions and the bond lengths in the allylium bridge indicating more stabilization of charge by the octamethylferrocenyl group.⁸ Electrochemical measurements also indicate that stabilization of positive charge in the series $[\text{Mc}(\text{CH})_3\text{Mc}]^+$ increases in the order Fc < Rc < Fc''.⁸ However, the extent to which these observations can be extended to chromophores in which neutral, but strong, acceptors are attached through π -conjugated bridges to a metallocenyl unit is unclear.

A large number of metallocene-based chromophores have been crystallographically characterized (in some cases with the aim of obtaining acentric crystals for nonlinear optical measurements or applications). However, in most cases these have been based on 4-nitrophenyl groups, or other groups with comparable or weaker π -accepting character, and the crystal structures have indicated ground-state geometries that are dominated by the neutral resonance structure. Although 4-nitrophenyl is often regarded as a rather strong π -acceptor, considerably stronger non-aromatic π -acceptors have been developed and incorporated into chromophores to afford much higher molecular nonlinearities; however, few crystal structure determinations have been published for chromophores incorporating these acceptors (Chart 1), i.e., for chromophores in which the zwitterionic resonance structure (Figure 1) might be expected to play a more significant role.^{9–11} There are also few crystal structures of ruthenocenyl dipolar chromophores^{12,13} and heavily methylated ferrocenyl^{14–18} dipolar chromophores; moreover, only in a limited number of these cases are the structures of the analogous unsubstituted ferrocenyl chromophores available for comparison.

Here we report the structures of six chromophores (**1–6**, Chart 2) in which ferrocenyl, octamethylferrocenyl, or ruthenocenyl donors are linked through a polyene bridge to the very strong non-aromatic 1,3-diethyl-2-thiobarbituric acid (TB) or 3-dicyanomethylidene-2,3-dihydrobenzothiophene-1,1-dioxide (SDS) acceptor groups and compare the crystallographic geometric data with information from NMR and IR spectroscopy, electrochemistry, and density functional theory (DFT) calculations. Large nonresonant values of $\mu\beta_{\mu}$, where μ is the dipole moment and β_{μ} is the projection of the first hyperpolarizability onto the dipole moment axis, have previously been measured for the ferrocenyl and ruthenocenyl chromophores (1900, 1000, 3000, and 1900×10^{-48} esu for **1**, **3**, **4**, and **6**, respectively, using electric-field-induced second-harmonic generation (EFISH) at $1.907 \mu\text{m}$ in CHCl_3),^{19,20} while one of the octamethylferrocenyl chromophores, **5**, was included in a Stark spectroscopy study demonstrating that two excited states make two-state contributions of comparable magnitude to the nonlinearity of metallocenyl chromophores.⁵

Experimental Details

Synthesis

The compounds were synthesized as previously described^{5,19,20} from reaction of the appropriate 5-metallocenylpenta-2,4-diene-1-yl, $\text{Mc}(\text{CH}=\text{CH})_2\text{CHO}$,^{5,19,20} with 1,3-diethyl-2-thiobarbituric acid, TB- H_2 (Aldrich), or 3-dicyanomethylidene-2,3-dihydrobenzothiophene-1,1-dioxide, SDS- H_2 .^{21,22}

Single-Crystal X-ray Structures

For all six compounds, crystals were obtained by slow evaporation of ethyl acetate solutions. Diffraction data were collected at 100(2) K with a Bruker SMART APEX II CCD area detector, using $\text{MoK}\alpha$ -radiation ($\lambda = 0.71073 \text{ \AA}$). Absorption corrections were applied using the semiempirical method SADABS,²³ except for the case of twinned crystal of compound **2**, for which TWINABS²⁴ was used instead. The structures were solved by direct methods and refined by full matrix least-squares on F^2 in the anisotropic approximation for non-hydrogen atoms. Hydrogen atoms were placed geometrically and included in refinement using a “riding” model with $U_{\text{iso}} = nU_{\text{eq}}$ for the carbon atom connected to the relevant H-atom where $n = 1.5$ for the hydrogen atoms in methyl groups and $n = 1.2$ for other hydrogen atoms. Data reduction and further calculations were performed using the Bruker SAINT²⁵ and SHELXTL NT program packages.²⁶ For crystal of compound **1**, highly disordered solvent molecules were found in the structure; therefore, the Platon “squeeze” option was applied in the refinement.²⁷ Selected refinement data and structure parameters, along with figures showing the numbering schemes for each structure, are presented in the Supporting Information. Complete crystallographic data are also provided in CIF format.

Electrochemistry

Cyclic voltammetry was carried out under nitrogen on dry deoxygenated dichloromethane solutions ca. 10^{-4} M in analyte and 0.1 M in tetra-*n*-butylammonium hexafluorophosphate using a BAS Potentiostat, a glassy carbon working electrode, a platinum auxiliary electrode, and, as a pseudo-reference electrode, a silver wire anodized in 1 M aqueous potassium chloride. Potentials were referenced to ferrocenium/ferrocene by using decamethylferrocene (-0.55 V vs. ferrocenium/ferrocene) as an internal standard. Cyclic voltammograms were recorded at scan rates of 50–1000 mVs^{-1} .

Spectroscopic Measurements

IR spectra were acquired as KBr discs using a Perkin-Elmer Spectrum 1000 spectrometer. ^1H and $^{13}\text{C}\{^1\text{H}\}$ NMR spectra were acquired in CD_2Cl_2 using a Bruker AMX-400 spectrometer.

Assignments of the spectra (see Supporting Information for full NMR data) were facilitated using COSY and HSQC 2D NMR experiments on Bruker AMX-400 and Bruker DRX-500 spectrometers, respectively.

DFT Calculations

DFT calculations were carried out using the B3LYP functionals, where Becke's three-parameter hybrid exchange functional is combined with the Lee-Yang-Parr correlation functional.^{28,29} The LANL2DZ basis set was used for Ru atoms and the 6-31G* basis set was used for all other atoms. All the calculations were done using the Gaussian 98 program.³⁰

Results

Crystallography and Molecular Geometry

Crystal structures for **1–6** were determined using single-crystal X-ray diffraction. As is typical for chromophores with large dipole moments, the structures of **1–6** belong to a centrosymmetric space group (in fact all belong to $P\bar{1}$), precluding bulk second-order nonlinear effects. To investigate the possibility that alternative NLO-active non-centrosymmetric polymorphs might be obtained under different conditions, we employed polymer-induced heteronucleation^{31,32} (PIHn) for the case of **3**, evaporating acetone solutions of in the presence of three polymer libraries. Although three distinct forms were identified using Raman spectroscopy and powder X-ray diffraction, the absence of a second harmonic generation signal suggested that none was non-centrosymmetric. These experiments, along with the crystal packing observed in the single-crystal structures of **1–6**, are discussed in the Supporting Information.

The molecular structures obtained from the single-crystal structure determinations are shown in Figure 2. In the case of **2**, there are two inequivalent molecules in the asymmetric unit, hereafter referred to as **2A** and **2B** (only **2A** is shown in Figure 2). In all the structures the π -systems are approximately planar from the substituted cyclopentadienyl ring of the donor to the plane of the acceptor heterocycle and, as expected, all-*E* configurations are observed for the CH—CH bonds of the polyene chains. The formally double $C_e—C_A$ bonds (see Figure 3 for definitions) of all three SDS chromophores have a *Z* configuration, i.e. with the donor-acceptor conjugation path running in a *trans* fashion. As discussed in the introduction, there are only a few previously reported crystal structures of metallocenyl dipolar chromophores with *very strong* non-aromatic organic acceptor groups. Significantly, the current series are the first in which one can directly compare the structures of analogous metallocenyl-polyene-acceptor chromophores with *three* different metallocenyl donors: ferrocenyl, heavily methylated ferrocenyl, and ruthenocenyl, while previous comparisons between even two types of donors are very limited.^{12,18,33}

The contribution of the zwitterionic resonance form to the ground-state structure of a donor-acceptor polyene can be gauged by the so-called bond-length alternation (BLA), defined here as the difference between the average lengths of the bonds of the polyene chain which are formally single in the neutral resonance form, and those which are double bonds.³⁴ Indeed, in simple organic polyenes the BLA has been correlated, both theoretically and experimentally, with the second-order nonlinearity.^{35–39} The BLA values calculated using all the C—C bonds between the metallocenyl group and the heterocycle of the acceptor (Table 2) fall in the range 0.054–0.072 Å (with similar values being found if the $C_{Mc}—C_\alpha$ and $C_e—C_A$ bonds, which are defined in Figure 3 and which might be influenced by steric as well as electronic effects, are excluded from the calculation); these values are similar to, though a little larger than, that obtained for the previously reported structure of an analogous chromophore with a ferrocenyl donor and the 3-dicyanomethylidene-1-indanone acceptor,¹¹ **III** (Chart 1, BLA = 0.049 Å). The pattern of alternation between individual bond lengths in **1–6** is a little more complex than

implied by the definition of an average BLA parameter: as in the structure of **III** (Chart 1)¹¹ and in crystallographically determined and theoretically calculated structures of several *p*-aminophenylpolyenes with strong heterocyclic acceptors,^{37,40} the BLA is more pronounced towards the donor end of the polyene chain.

The average BLA parameters for **1–6** and the closely analogous **III**¹¹ indicate significant contribution from zwitterionic resonance forms in metallocenyl chromophores of this type with very strong non-aromatic π -acceptors. In polyenes without significant donor/acceptor π -interaction,^{41–46} including ferrocenyl-terminated examples,⁴⁷ typical bond-length alternations are 0.10–0.12 Å. Indeed, ferrocenyl-polyene-acceptor chromophores incorporating the aromatic *p*-nitrophenyl π -acceptor, which although a strong acceptor is considerably weaker than TB and SDS, also exhibit crystallographic BLAs of over 0.1 Å,⁴⁸ while Fc (CH=CH)₃CHO shows a BLA of 0.09 Å.⁴⁹ The variations in BLAs between SDS chromophores and their TB analogues, or between chromophores with different metallocenyl donors, are of the same magnitude as the estimated standard deviations (esds) in the individual bond lengths and, therefore, the crystallographic evidence does not allow us to rank the different donors in order of π -donor strength, or to compare the π -acceptor strengths of TB and SDS.⁵⁰

The BLAs observed for **1–6** approach the value (ca. 0.05 Å, depending on the chain length) corresponding to maximum positive values of the second-order polarizability, β , in organic polyenes,^{35–39} although it is not clear that the β -BLA relationships that have been discussed in the literature are directly applicable to metallocenyl species. In addition, dipolar chromophores are sensitive to the polarity of the surrounding medium, with high polarity media favoring reduced BLA;^{36,38,51} crystals of this type of chromophore are highly polar media and so higher BLAs might be anticipated in solvents of low to moderate polarity or in the gas phase. However, geometric parameters for gas-phase **1–6** obtained from DFT calculations show remarkably good agreement with the crystallographic data (Table 1); calculated BLAs fall in the range 0.054–0.063 Å and the experimentally observed decreases in BLA from donor to acceptor end of the polyene chain are reproduced.⁵² Differences in the DFT bond lengths and BLAs between different molecules, which would be too small to be reliably detected in crystallographic data, do, however, show distinct trends, suggesting that the degree of ground-state charge-transfer increases in the order Fc < Rc \ll Fc'' and TB < SDS.

The BLAs for **1–6** can also be compared to all-organic chromophores incorporating the same acceptor moieties. For the TB-based chromophore **VIII** (Chart 3), the BLA is close to zero (–0.01 Å) indicating that charge-separated and neutral resonance structures make approximately equal contributions to the ground-state structure,³⁸ and indicating that dialkyl amines directly attached to the polyene chain are much stronger π -donors than metallocenes. Chromophore **IX** (Chart 3) exhibits greater BLA (ca. 0.04 Å)⁴⁰ than **VIII** due to the aromaticity of the phenylene ring resisting contributions from the zwitterionic form. Although the experimental BLA in **IX** is slightly lower than in the analogous metallocenyl chromophores **4–6**, suggesting *p*-aminophenyl groups act as stronger π -donors than metallocenyl groups with this type of acceptor, the DFT geometries suggest that *p*-ⁿBu₂NC₆H₄ exhibits a very similar π -donor strength to Fc'' (calculated BLA of 0.055 Å).⁵³

Although, as discussed above, the BLAs in the polyene bridges of **1–6** indicate significant contributions from zwitterionic resonance forms, this contribution is accompanied by negligible distortions of the metallocenyl donors towards the $[\eta^6\text{-fulvene}]CpM]^+$ extreme (Figure 1b–ii). The geometric parameters defined in Figure 1c all fall within the ranges found for the appropriate “undistorted” metallocenes. For example, unmethylated $[\eta^6\text{-fulvene}]CpRu]^+$ derivatives exhibit values of the Ru–C $_{\alpha}$ bond lengths and β in the ranges 2.251–2.604 Å and 28.2–42.6 °,^{6–8,54–57} respectively, whereas the corresponding values for **3** (3.194 Å, 1.2 °) and **6** (3.162 Å, 3.1 °) are typical for “normal” ruthenocenes. Similarly, the Fe–C $_{\alpha}$ and

β values for Fc'' chromophores **2A** (3.317 Å, 2.0 °), **2B** (3.315 Å, 3.0 °) and **5** (3.098 Å, 0.8 °) are within the range for "normal" metallocenes, and are far from the values of 2.567 Å and 23.6 °, respectively, for $[(\eta^6\text{-C}_5\text{Me}_4\text{CH}_2)(\eta^5\text{-C}_5\text{Me}_5)\text{Fe}]^+$.⁵⁸ Appropriate comparisons for the Fc-based chromophores **1** (3.106 Å, 2.0 °) and **4** (3.070 Å, 3.9 °) are less readily available due to the instability of simple ferrocenyl carbocations;⁵⁹ however, even in a species such as $[\text{FcCPh}_2]^+$, where the Ph groups also stabilize the positive charge, Fe—C $_{\alpha}$ and β values are 2.715 Å and 20.7 °, respectively.⁶⁰ The DFT structures also show little distortion of the metallocenes from "normal" geometry. However, while the experimental and calculated structures of **1–6** and the closely related polyene **III** (Chart 1)¹¹ show very limited distortions from ideal metallocene geometry, for **1** β is as high as 10.2 ° and Fe—C $_{\alpha}$ falls to 2.954 Å,⁹ indicating that the extent to which the $[(\eta^6\text{-fulvene})\text{CpM}]^+$ resonance form contributes to the structure depends on the polyene chain length in addition to the identity of the acceptor. This observation, along with the decreased BLA seen towards the acceptor end of the polyene, as discussed above for **1–6** and **III**, and the calculated partial charges (see below), indicates that the polyene bridging group, as well as the metallocene itself, can act as donor towards the heterocyclic acceptor.⁶¹ Moreover, the lowest-lying empty orbitals of **1–6**, as in those of *p*-nitrostyryl derivatives,⁵ are located towards the acceptor end of the polyene chains,⁶² precluding direct overlap with a filled metal orbital.

NMR Spectroscopy

In addition to crystallography, other techniques may be used to gain insight into the degree of ground-state charge transfer in chromophores of this type. ¹H NMR spectra (see Supporting Information for complete NMR data) confirm some of the features observed crystallographically and in the DFT structures; the coupling constants associated with the polyene bridging units, determined in CD₂Cl₂ (Table 2), are consistent with some reduction in BLA relative to an ideal polyene, for which typical coupling constants are 16 and 10 Hz across *trans* double and single bonds, respectively.⁶³ Moreover, the coupling constants are also consistent with more pronounced BLA at the donor ends of the polyene chains than the acceptor ends. Fc and Rc analogues show essentially the same coupling constants as one another (**1** vs. **3**; **4** vs. **6**). All the measurable coupling constants for the Fc'' chromophore **5** suggest more ground-state charge transfer than in its Fc (**4**) and Rc (**6**) analogues and even slightly more than for its all-organic compound **IX**, while the comparison of **1** vs. **2** and **3** is less clearcut. The comparison between TB and SDS acceptors (**1** and **3** vs. **4** and **6**, respectively) is also less straightforward, with the coupling constants across the formally single bonds, in particular, suggesting greater BLA in the SDS chromophores, in contrast to the computational geometries (*vide supra*) and to other NMR and computational evidence (*vide infra*) suggesting SDS is the stronger of the two π acceptors (the energies of charge-transfer-type absorptions 5.19·20·40 and the electrochemical data discussed below certainly suggest that SDS is the stronger acceptor in an electron-transfer sense).

In particular, ¹³C NMR chemical shifts (see Supporting Information for complete NMR characterization) suggest SDS to be a slightly stronger acceptor than TB; for example, the ¹³C resonances corresponding to the ruthenocenyl methine nuclei of **6** are each observed ca. 0.3–0.6 ppm downfield of those in **3** (the quaternary ruthenocenyl resonance is seen at the same chemical shift within experimental error), with similar behavior also seen for the Fc and Fc'' chromophores. The chemical shift of the C₅H₅ ¹H and ¹³C resonances of the Fc and Rc chromophores can also be compared to those in the parent metallocenes: the similarity in the chemical shift differences between Fc and Rc chromophores and the respective parent metallocenes further supports the similarity of Fc and Rc as π -donors in this type of chromophore. The chemical shifts of the metallocenyl resonances are also consistent with minimal distortion of the donors towards the $[(\eta^6\text{-fulvene})\text{CpM}]^+$ structure; the ¹³C chemical shifts for the C₅H₅ resonances of **3** (72.3 ppm) and **6** (72.6 ppm) are much closer to that for

ruthenocene (70.6 ppm) than to those for $[\text{RcCH}_2]^+$ salts in the same solvent (84.1–84.5 ppm).
57

The ^{13}C shifts for atoms in the acceptor groups on which one can place a negative charge in reasonable zwitterionic resonance structures are expected to be the most sensitive to variation in the donor groups. Accordingly, the resonance corresponding to C_A (Figure 3) of the TB acceptor varies from 113.05 and 113.17 ppm for Fc and Rc chromophores **1** and **3**, respectively, to 110.69 ppm for the Fc'' chromophore **2**, suggesting that the charge density at this nucleus and, therefore, the π -donor strengths increase in the order $\text{Rc} \sim \text{Fc} < \text{Fc}''$, while the CO and CS ^{13}C chemical shifts are relatively insensitive to the identity of the donor.⁶⁴

Electrochemistry

Electrochemical potentials also offer information regarding donor-acceptor interactions. Compounds **1–6** were studied using cyclic voltammetry in $\text{CH}_2\text{Cl}_2/0.1 \text{ M } ^n\text{Bu}_4\text{NPF}_6$; potentials are summarized in Table 4 and representative voltammograms are shown in Figure 9. Values in $\text{THF}/0.1 \text{ M } ^n\text{Bu}_4\text{NPF}_6$ have previously been reported.⁵ The Fc and Fc'' chromophores exhibit reversible features corresponding to the $+0$ couple, while the Rc chromophores undergo completely irreversible molecular oxidations, as does ruthenocene itself.⁶⁵ The $0/-$ couples are in all cases of EC type, i.e. are reversible electron transfer processes followed by chemical reaction on timescales comparable to the scan rate; those for the SDS chromophores are generally more reversible than those of their TB analogues and the $0/-$ couple for the Fc'' -SDS example **5** approaches full reversibility at high scan rates (see Figure 9a). The $+0$ couples clearly suggest more ground-state charge transfer in the Fc'' chromophores than in their Fc analogues: the potentials for **2** and **5** are shifted to more oxidizing potential than that of the parent metallocene, 1,2,3,4,1',2',3',4'-octamethylferrocene, by 0.20 and 0.24 V, respectively, whereas those of **1** and **4** are shifted from that of ferrocene by 0.16 and 0.15 V, respectively. The $0/-$ couples also indicate Fc'' chromophores are 0.07–0.13 V less readily reduced than their Fc analogues, also consistent with greater ground-state charge transfer in the Fc'' compounds. On the other hand, Rc compounds are reduced at similar potential to their Fc analogues, implying that Fc and Rc chromophores exhibit similar degrees of ground-state charge-transfer. Thus, these results are in line with the DFT geometrical data discussed above. The differences between $+0$ potentials for TB and SDS chromophores are of questionable significance. Comparison of $0/-$ potentials suggests that **IX** lies intermediate between Fc and Fc'' analogues **4** and **5** in the degree of ground-state charge-transfer in solution, in contrast to crystallographic data indicating **IX** exhibits lower BLA, at least in the crystal.

Vibrational Spectroscopy

The acceptor groups used in both TB and SDS chromophores contain functional groups exhibiting distinctive IR-active stretches. In particular, the $\text{C}\equiv\text{N}$ stretching frequencies, ν_{CN} , for SDS-based compounds are well-separated from those of other vibrations. Although, in principle, two distinct stretches are expected for each species, one band is seen with a poorly defined shoulder on the low-frequency side; the band maxima are collected in Table 4. In the donor-acceptor compounds ν_{CN} is reduced relative to that in the parent acceptor, dicyanomethylidene-2,3-dihydrobenzothiophene-1,1-dioxide, SDS- H_2 ; this can be attributed to contributions from charge-separated resonance forms. The frequencies also suggest that the degree of charge separation is similar in Fc and Rc chromophores, **4** and **6**, respectively, while a greater degree of separation is present in the Fc'' chromophore, **5**, and in the all-organic analogue, **IX**. In the TB chromophores, a strong, somewhat broad, band is seen at ca. 1650 cm^{-1} . Since no strong features are seen at $\nu > 1600 \text{ cm}^{-1}$ in the SDS chromophores, this feature can be attributed to the $\text{C}=\text{O}$ stretching modes, ν_{CO} . The data, which are shown in Table 4, suggest that the degree of charge separation decreases in the order $\text{Fc}'' > \text{Rc} \sim \text{Fc}$.

Calculated Charge Densities

The DFT calculations were also used to obtain information regarding the charge distribution in the chromophores; in Table 5 the atomic (Mulliken) charges are summed over donor, π -bridge, and acceptor portions of each chromophore (tables of the individual atomic charges are shown in the Supporting Information). Inspection of the atomic charge totals for the donor portion are clearly consistent with a π -donor order of p -ⁿBu₂NC₆H₄ > Fc'' > Rc > Fc and a π -acceptor order of SDS > TB.⁶⁷ The total acceptor charges indicate similar conclusions, although, surprisingly, the TB acceptors of Fc'' compound **2** and Rc compound **3** bear essentially the same charge. In all the chromophores examined, the polyene bridge bears a net positive charge implying that the bridge acts as a net donor in these particular systems. The magnitude of the bridge charge does not vary in a particularly straightforward way with donor, although consistently more donation from the bridge is observed in SDS chromophores than in their TB analogues, apparently at variance with ¹³C NMR chemical shift data for the polyene atoms of the bridge, which suggest the bridges of the TB chromophores to be more electron-poor than those of the SDS chromophores.^{68,69}

Discussion and Conclusion

The polyene bridges in the crystal structures of **1–6** are characterized by considerably reduced BLA relative to simple polyenes. However, the differences in π -donor strength between Fc, Fc'', and Rc (and in π -acceptor strength between TB and SDS) are insufficient to result in crystallographically detectable variation in the BLA between the different chromophores. However, DFT calculations (both geometries and partial charges) and data from NMR, electrochemical, and IR measurements concur to indicate that in these systems Fc'' is a considerably stronger π -donor than Fc or Rc and is similar in π -donor strength to a p -(dialkylamino)phenyl group. In this series of chromophores, Fc and Rc are very similar in π -donor strength, with computational data indicating Rc to be a slightly stronger donor. The superior π -donor strength of Fc'' parallels the known effect of methylation on the electron-transfer strength (ease of ionization) of ferrocenes (the gas-phase ionization potential of FeCp*₂ is ca. 1.0 eV lower than that of FeCp₂;³ numerous electrochemical studies^{70–72} indicate methylated ferrocenes are more readily oxidized than FeCp₂). However, the similarity in π -donor strength for Fc and Rc can be contrasted to the very different electron-transfer donor strengths indicated by the gas-phase vertical ionization potentials of the parent metallocenes (FeCp₂ is ca. 0.6 eV more easily ionized than RuCp₂).^{3,4} To understand this discrepancy, it should be realized that the highest occupied orbitals of metallocenes are essentially metal-based d-orbitals which can couple only weakly to an attached π -system, at least in the case of weakly accepting π -systems. However, the energies of the highest ligand-based orbitals, which are known to couple strongly to attached π -systems in π -nitrostyryl derivatives,⁵ are sensitive to methylation, but relatively insensitive to the identity of the metal; values of 8.7, 7.3, and 8.5 eV have been assigned to the first ligand-based ionizations of FeCp₂, FeCp*₂ and RuCp₂, respectively,^{3,4} this pattern being consistent with the order of π donor strengths observed in the present series of of Mc(CH=CH)₂CH=A chromophores with strong neutral heterocyclic acceptors, i.e., Fc'' \gg Rc \geq Fc.

Both crystallographic and computational geometries indicate little contribution from the [(η^6 -fulvene)CpM]⁺ resonance form in **1–6**, consistent with the crystal structure of **III**,¹¹ but in contrast to that of **I**,⁹ in which the bridging CH group is clearly bent towards the metal atom. The similarity in π -donor strengths of Fc and Rc found in the present compounds is at variance with previous cationic examples where the [(η^6 -fulvene)CpM]⁺ structure type dominates and where Rc is a much stronger π donor,^{6,8} presumably due to the role played by the more diffuse 4d orbitals of ruthenium in facilitating coordination to the bridging carbon atom.⁷³ Clearly then the relative π -strengths of different metallocenyl groups cannot be defined in one simple straightforward way, with the nature of the π -bridge and the acceptor appearing to play a role.

Finally, it is worth pointing out that the π -donor strengths discussed here do *not* correlate directly with the linear and nonlinear optical properties of these chromophores since these both metal-to-acceptor states (the energy of which varies according to the electron-donor strengths of the metallocenes) and π -to-acceptor states (which depend largely on the π -donor strengths) contribute significantly.^{5,62} However, a better understanding of the π donor strengths of metallocenes may help with the design of metallocene-substituted π -systems for particular applications or to address specific questions.

Supplementary Material

Refer to Web version on PubMed Central for supplementary material.

Acknowledgments

This material is based upon work supported in part by the STC Program of the National Science Foundation under Agreement Number DMR-0120967. We also thank the National Institute of Health for funding through the RIMI program (award number 1P20MD001104-01). We also thank Les Gelbaum for recording HSQC 2D spectra, Greg Walker for a sample of **IX**, and Marcin Palusiak for help finding crystallographic data for compound **III**.

References

1. Thompson, ME.; Djurovich, PE.; Barlow, S.; Marder, SR. *Comprehensive Organometallic Chemistry III*. O'Hare, D.; Crabtree, R.; Mingos, M., editors. Vol. 12. Elsevier; Oxford: 2006.
2. Barlow S, Marder SR. *Chem Commun* 2000:1555.
3. Cauletti C, Green JC, Kelly MR, Robbins J, Smart JC. *J Electron Spectrosc Relat Phenom* 1980;19:327.
4. Evans S, Green MLH, Jewitt B, Orchard AF, Pygall CF. *J Chem Soc, Faraday Trans 2* 1972;68:1847.
5. Barlow S, Bunting HE, Ringham C, Green JC, Bublitz GU, Boxer SG, Perry JW, Marder SR. *J Am Chem Soc* 1999;121:3715.
6. Watanabe M, Motoyama I, Takayama T. *Bull Chem Soc Jpn* 1996;69:2877.
7. Watanabe M, Motoyama I, Takayama T. *J Organomet Chem* 1996;524:9.
8. Barlow S, Henling LM, Day MW, Schaefer WP, Green JC, Hascall T, Marder SR. *J Am Chem Soc* 2002;124:6285. [PubMed: 12033856]
9. Janowska I, Zakrzewski J, Nakatani K, Delaire JA, Palusiak M, Walak M, Scholl H. *J Organomet Chem* 2003;675:35.
10. Liao Y, Eichinger BE, Firestone KA, Haller M, Luo J, Kaminsky W, Benedict JB, Reid PJ, Jen AKY, Dalton LR, Robinson BH. *J Am Chem Soc* 2005;127:2759.
11. Janowska I, Zakrzewski J, Nakatani K, Palusiak M, Walak M, Scholl H. *J Organomet Chem* 2006;691:323. (see CCDC269208 for structural details).
12. Wong H, Meyer-Friedrichsen T, Farrell T, Mecker C, Heck J. *Eur J Inorg Chem* 2000;2000:631.
13. Meyer-Friedrichsen T, Wong H, Prosenc MH, Heck J. *Eur J Inorg Chem* 2003:936.
14. Hradsky A, Bildstein B, Schuler N, Schottenberger H, Jaitner P, Ongania KH, Wurst K, Launay JP. *Organometallics* 1997;16:392.
15. Malaun M, Kowallick R, McDonagh AM, Marcaccio M, Paul RL, Asselberghs I, Clays K, Persoons A, Bildstein B, Fiorini C, Nunzi JM, Ward MD, McCleverty JA. *J Chem Soc, Dalton Trans* 2001:3025.
16. Malaun M, Reeves ZR, Paul RL, Jeffrey JC, McCleverty JA, Ward MD, Asselberghs I, Clays K, Persoons A. *Chem Commun* 2001:49.
17. Sporer C, Ratera I, Ruiz-Molina D, Zhao Y, Vidal-Gancedo J, Wurst K, Jaitner P, Clays K, Persoons A, Rovira C, Veciana J. *Angew Chem Int Ed* 2004;43:5266.
18. Laus G, Schottenberger H, Wurst K, Herber RH, Griesser U. *J Phys Chem B* 2004;108:5082.
19. Alain V, Blanchard-Desce M, Chen CT, arder SR, Fort A, Barzoukas M. *Synth Met* 1996;81:133.
20. Alain V, Fort A, Barzoukas M, Chen CT, Blanchard-Desce M, Marder SR, Perry JW. *Inorg Chim Acta* 1996;242:43.

21. Baumann, W. French Patent, *FR 2438045*, 1980.
22. Shenoy VU, Patel VP, Seshadri S. *Dyes Pigm* 1989;11:37.
23. Sheldrick, GM. SADABS v.2.03, Bruker/Siemens Area Detector Absorption Correction Program. Bruker AXS: Madison, WI, USA; 2003.
24. Sheldrick, GM. TWINABS. Bruker AXS: Madison, WI; 2002.
25. SAINTP+ for NT, v.6.2, Data Reduction and Correction Program. Bruker AXS; Madison, WI, USA: 2001.
26. Sheldrick, GM. SHELXTL NT v. 6.12, Structure Determination Software Suite. Bruker AXS; Madison, WI, USA: 2001.
27. Spek, AL. PLATON — A Multi Purpose Crystallographic Tool. Utrecht University; Utrecht, The Netherlands: 2002.
28. Becke AD. *J Chem Phys* 1993;98:5648.
29. Lee CT, Yang WT, Parr RG. *Phys Rev* 1988;B37:785.
30. Frisch, MJ.; Trucks, GW.; Schlegel, HB.; Scuseria, GE.; Robb, MA.; Cheeseman, JR.; Zakrzewski, VGJAM., Jr; Stratmann, RE.; Burant, JC.; Dapprich, S.; Millam, JM.; Daniels, AD.; Kudin, KN.; Strain, MC.; Farkas, O.; Tomasi, J.; Barone, V.; Cossi, M.; Cammi, R.; Mennucci, B.; Pomelli, C.; Adamo, C.; Clifford, S.; Ochterski, J.; Petersson, GA.; Ayala, PY.; Cui, Q.; Morokuma, K.; Salvador, P.; Dannenberg, JJ.; Malick, DK.; Rabuck, AD.; Raghavachari, K.; Foresman, JB.; Cioslowski, J.; Ortiz, JV.; Baboul, AG.; Stefanov, BB.; Liu, G.; Liashenko, A.; Piskorz, P.; Komaromi, I.; Gomperts, R.; Martin, RL.; Fox, DJ.; Keith, T.; Al-Laham, MA.; Peng, CY.; Nanayakkara, A.; Challacombe, M.; Gill, PMW.; Johnson, B.; Chen, W.; Wong, MW.; Andres, JL.; Gonzalez, C.; Head-Gordon, M.; Replogle, ES.; Pople, JA. Gaussian 98 (Revision A.11.1). Gaussian, Inc.; Pittsburgh PA: 2001.
31. Lang MD, Grzesiak AL, Matzger AJ. *J Am Chem Soc* 2002;124:14834. [PubMed: 12475310]
32. Price CP, Grzesiak AL, Matzger AJ. *J Am Chem Soc* 2005;127:5512. [PubMed: 15826189]
33. Comparisons of the structures of $\text{FeCH}=\text{C}(\text{CN})_2$ (Krukoni AP, Silverman J, Yannoni NF. *Acta Crystallogr* 1972;B28:987.) and $\text{Fe}^{\text{II}}\text{CH}=\text{C}(\text{CN})_2$ (reference 18) are not very informative regarding the electronic effects of ferrocene methylation since the π -system of the latter chromophore is severely distorted from planarity due to steric interference between methyl and cyano groups.
34. In some of the literature, for example reference ³⁵, BLA has been defined in the opposite sense, so that structures in which the neutral limiting form dominates have negative BLA.
35. Gorman CB, Marder SR. *Proc Natl Acad Sci USA* 1993;90:11297. [PubMed: 11607441]
36. Marder SR, Gorman CB, Meyers F, Perry JW, Bourhill G, Brédas JL, Pierce BM. *Science* 1994;265:632. [PubMed: 17752759]
37. Marder SR, Cheng LT, Tiemann BG, Friedli AC, Blanchard-Desce M, Perry JW, Skindhøj J. *Science* 1994;263:511. [PubMed: 17754885]
38. Bourhill G, Brédas JL, Cheng LT, Marder SR, Meyers F, Perry JW, Tiemann BG. *J Am Chem Soc* 1994;116:2619.
39. Meyers F, Marder SR, Pierce BM, Brédas JL. *J Am Chem Soc* 1994;116:10703.
40. Blanchard-Desce M, Alain V, Bedworth PV, Marder SR, Fort A, Runser C, Barzoukas M, Lebus S, Wortmann R. *Chem Eur J* 1997;3:1091.
41. Rabinovich D, Shakked Z. *Acta Crystallogr* 1975;B31:819.
42. Hall T, Bachrach SM, Spangler CW, Sapochak LS, Lin CT, Gwen HW, Rogers RD. *Acta Crystallogr* 1989;C45:1541.
43. Zhong JC, Munakata M, Kuoda-Sowa T, Maekawaw M, Suenaga Y, Konaka H. *Inorg Chim Acta* 2001;322:150.
44. Glaser R, Dendi LR, Knotts N, Barnes CL. *Cryst Growth Des* 2003;3:291.
45. Sonoda Y, Kawaniski Y, Goto M. *Acta Crystallogr* 2003;C59:o311.
46. Sonoda Y, Kawaniski Y, Goto M. *Acta Crystallogr* 2005;E61:1200.
47. Yuan P, Liu SH, Xiong W, Yin J, Yu G, Sung HY, Williams ID, Jia G. *Organometallics* 2005;24:1452.
48. Togni A, Rihs G. *Organometallics* 1993;12:3368.
49. Liu J, Castro R, Abboud KA, Kaifer AE. *J Org Chem* 2000;65:6973. [PubMed: 11031018]

50. The authors of reference ¹⁰ have suggested that the C₅H₅ ring of ferrocenyl donors is contracted by the influence of acceptor groups and that the degree of this contraction increases with acceptor strength. However, there is little evidence for such a correlation between the C₅H₅ C—C bond length and acceptor strength in the present structures or among literature structures (including both derivatives without acceptors and examples with directly attached carbocations such as [FcCPh₂]⁺ (reference 60). The apparent trend within the structures of reference 10 may be due to artefacts associated with modeling the thermal parameters in the C₅H₅ rings.
51. Dehu C, Meyers F, Hendrickx E, Clays K, Persoons A, Marder SR, Brédas JL. *J Am Chem Soc* 1995;117:10127.
52. It has been pointed out that the properties of polyene-like systems are not always perfectly reproduced by DFT methods (for example: (a) Cai ZL, Sendt K, Reimers JR. *J Chem Phys* 2002;117:5543. (b) Jacquemin D, Femenias A, Chermette H, Ciofini I, Adamo C, André JM, Perpète EA. *J Phys Chem A* 2006;110:5952. [PubMed: 16640395] In particular, many DFT functionals, including B3LYP, underestimate BLA in polar polyene systems (reference 52b). Thus, underestimation by the DFT calculations of the gas-phase BLA values may result in fortuitous agreement with experimental crystallographic values.
53. Previously reported AM1 calculations suggest a larger BLA of 0.090 Å for IX (see reference 40).
54. Sato M, Kawata Y, Kudo A, Iwai A, Saitoh H, Ochiai S. *J Chem Soc, Dalton Trans* 1998:2215.
55. Sato M, Iwai A, Watanabe M. *Organometallics* 1999;18:3208.
56. Barlow S, Day MW, Marder SR. *Acta Crystallogr* 2000;C56:303.
57. Barlow S, Cowley AR, Green JC, Brunner TJ, Hascall T. *Organometallics* 2001;20:5351.
58. Kreindlin AZ, Dolgushin FM, Yanovsky AI, Kerzina ZA, Petrovskii PV, Rybinskaya MI. *J Organomet Chem* 2000;616:106.
59. Rinehart KL, Michejda CJ, Kittle PA. *J Am Chem Soc* 1959;81:3162.
60. Behrens U. *J Organomet Chem* 1979;182:89.
61. This is consistent with our previously reported DFT study of *E*-(4-nitrostyryl)ferrocene (reference 8) in which the HOMO–3 can be described as an out-of-phase combination of the a cyclopentadienyl-based orbital and the highest molecular orbital of the ethylene bridge.
62. The calculated molecular orbitals of these chromophores will be discussed in detail elsewhere, along with a theoretical analysis of their optical properties.
63. Pretsch, E.; Bühlmann, P.; Affolter, C. *Structure Determination of Organic Compounds*. Springer-Verlag; Berlin: 2000.
64. In the SDS series, C_A was less unambiguously identified. However, the peaks seen at 124.55, 128.16, and 125.68 ppm for 5, 6 and IX, respectively, are tentatively assigned to C_A, and suggest R_c << *p*-ⁿBu₂NC₆H₄ < Fc'' in π-donor strength. The C(CN)₂ resonances, C_C, were only observed for 6 and IX, and also suggest *p*-ⁿBu₂NC₆H₄ < Fc''.
65. Diaz AF, Mueller-Westerhoff UT, Nazzari A, Tanner M. *J Organomet Chem* 1982;236:C45.
66. Barlow S. *Inorg Chem* 2001;40:7047. [PubMed: 11754289]
67. Although it may be tempting to compare the calculated differences in the partitioning of charge between donor, bridge, and acceptor with experimentally determined dipole moments available for 1 and 4 (reference 19), one should bear in mind that, in addition to the donor-acceptor charge separation, local dipoles associated with portions of the acceptor group also make substantial contributions to the ground-state dipole. However, it is worth noting that experimental dipole moments of 4.4 and 5.3 × 10⁻¹⁸ esu for *E*-4-nitrostyryl derivatives of ferrocene and ruthenocene, respectively, may be indicative of increased charge separation in the Ru species (Calabrese JC, Cheng LT, Green JC, Marder SR, Tam W. *J Am Chem Soc* 1991;113:7227.
68. ¹³C shifts of are known to be inversely correlated with the π electron density at that carbon ((a) Spiess H, Schneider WG. *Tetrahedron Lett* 1961:468. (b) Gunther H, Prestein J, Josephnathan P. *Org Magn Res* 1975;7:339. (c) Farnum DG. *Adv Phys Org Chem* 1975;11:123. (d) Sterk H, Holzer HZ. *Naturforsch* 1974;A29:974. (e) Sterk H, Fabian W. *Org Magn Res* 1975;7:274. (f) Reimers JR, Craw JS, Hush NS. *J Phys Chem* 1993;97:2778.
69. The chemical shifts associated with the polyene carbons of the present chromophores (assigned in the Supporting Information) are consistent with an alternating pattern of charge distribution for a donor-acceptor polyene, with higher electron density (more negative charge density) on the β and

δ -C atoms (at which one can place a negative charge in zwitterionic resonance structures with a donor-localized positive charge) than at the α , γ and ϵ -C atoms (at which one can place a positive charge in zwitterionic structures in which the negative charge is localized on A). The calculated atomic charge densities (given for all atoms in the Supporting Information) suggest a less clear-cut pattern; however, it should be realized that these values are the sum of π and σ electron density and may be more significantly affected by inductive effects than the ^{13}C chemical shifts.

70. Hoh GLK, McEwen WE, Kleinberg J. *J Am Chem Soc* 1961;83:3949.
71. Robbins JL, Edelstein N, Spencer B, Smart JC. *J Am Chem Soc* 1982;104:1882.
72. Gassman PG, Macomber DW, Hershberger JW. *Organometallics* 1983;2:1470.
73. Electrochemical measurements suggest that the stabilization of positive charge in the series $[\text{Mc}(\text{CH}_3)_3\text{Mc}]^+$ is greater when $\text{Mc} = \text{Rc}$ (reference 8). Together with the crystallographic data for compounds of this type (references 6 and 8), this behavior is consistent with other features of the chemistry of the group 8 metals in which Ru shows tendencies to adopt higher coordination numbers, increased covalency, and higher oxidation states (note that Figure 1c–iii represents a M^{IV} limiting form) than Fe.

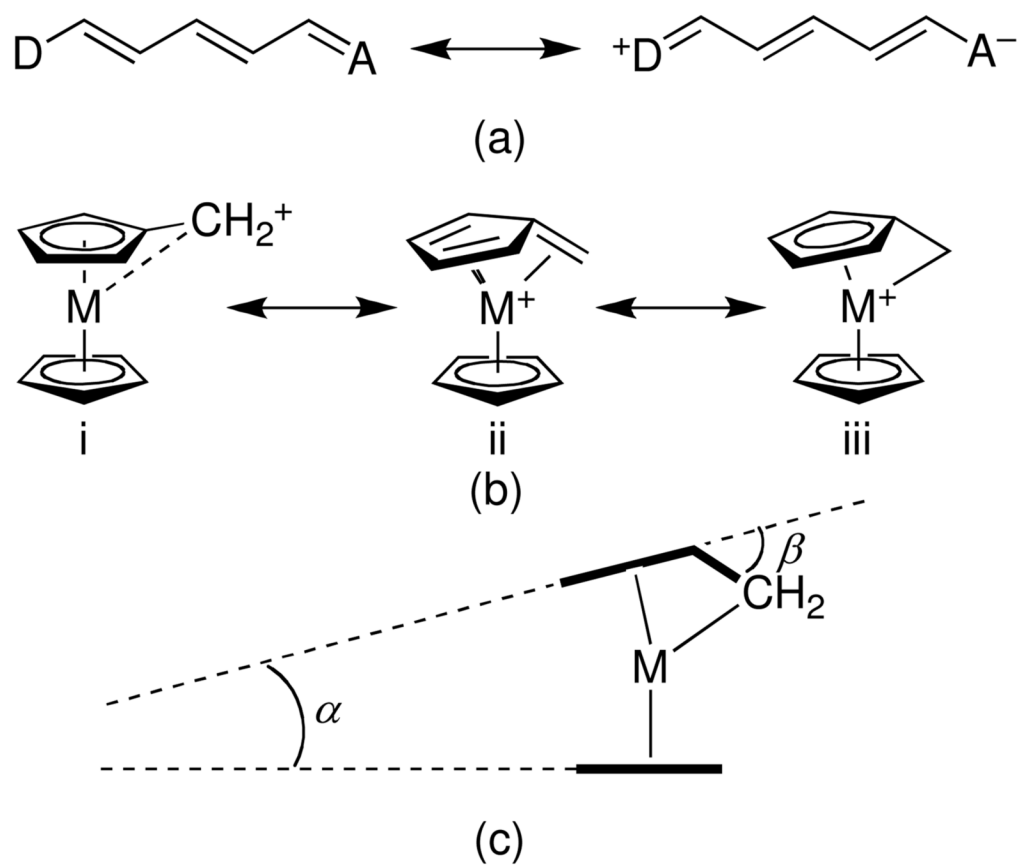


Figure 1. (a) Neutral and zwitterionic resonance structures for a donor-(conjugated bridge)-acceptor polyene; (b) resonance structures contributing to the stabilization of metalocenyl carbocations; and (c) definition of angles quantifying structural distortions in metalocenyl carbocations.

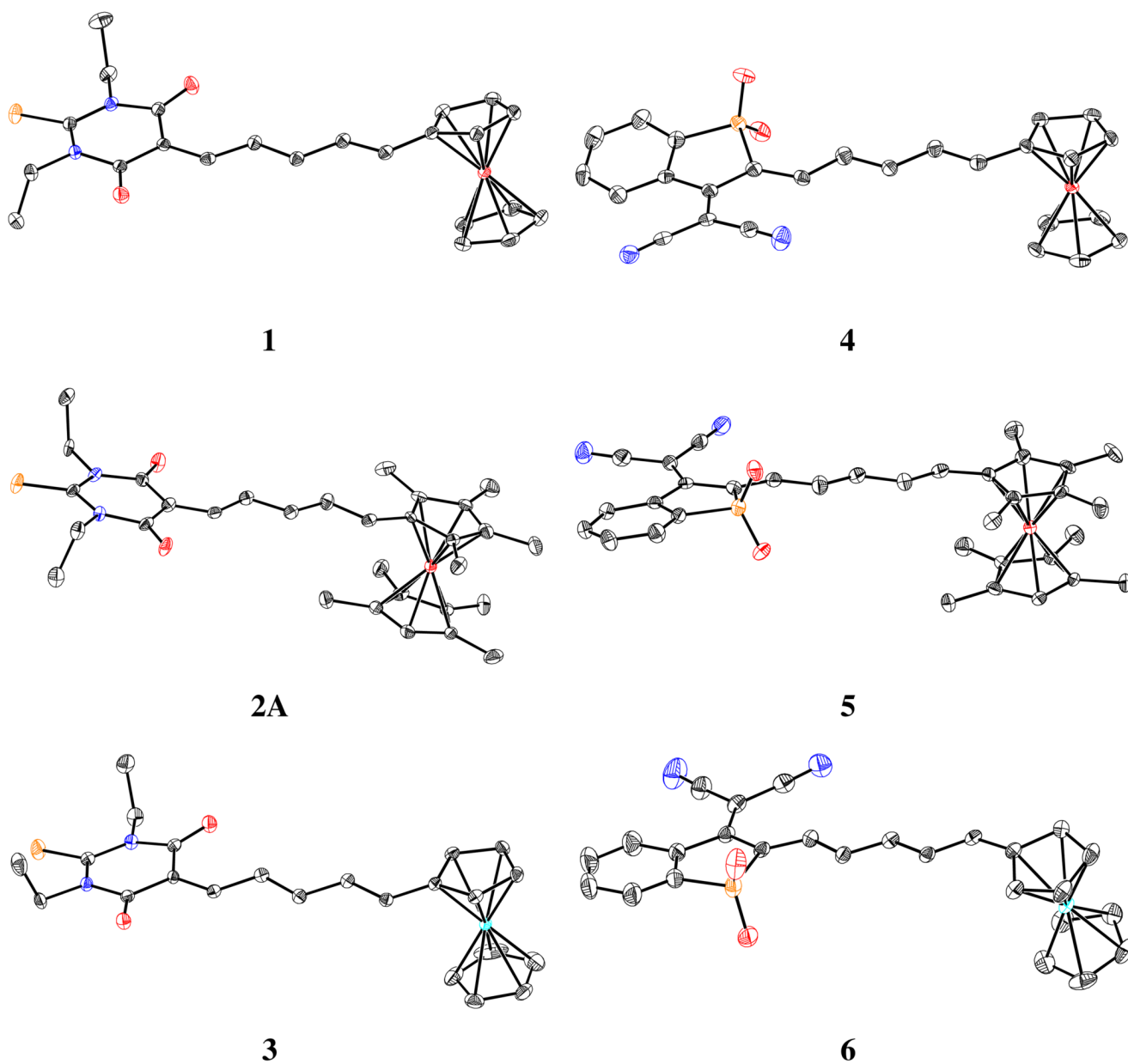


Figure 2. Views of molecules **1–6** in their crystal structures (50% thermal ellipsoids). Molecule **2B** is similar to molecule **2A** and is shown in the Supporting Information along with atom numbering schemes for all molecules. Carbon atoms are shown in black, sulfur in yellow, nitrogen in blue, oxygen and iron in red, and ruthenium in pale blue.

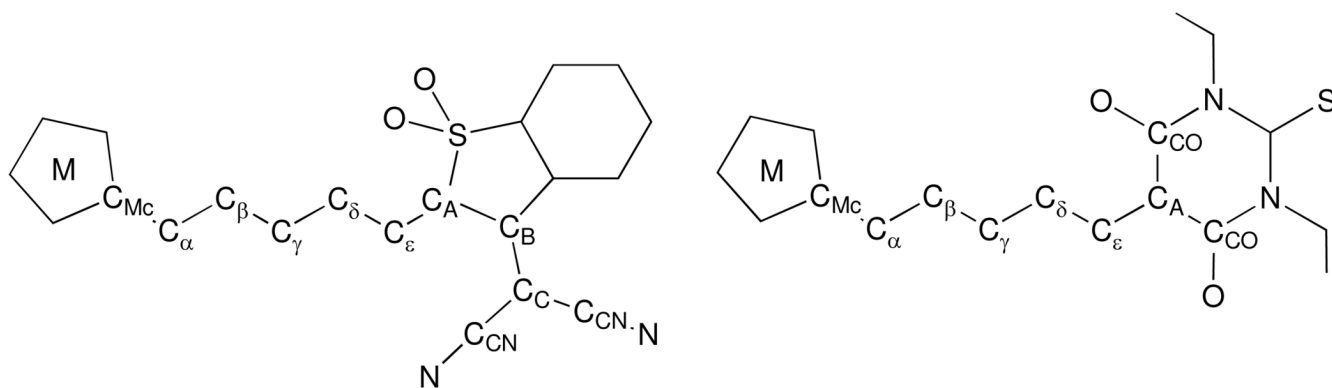


Figure 3. Definition of generalized atom labels used to define the bond lengths compared in Table 1 and in discussion of X-ray and NMR data.

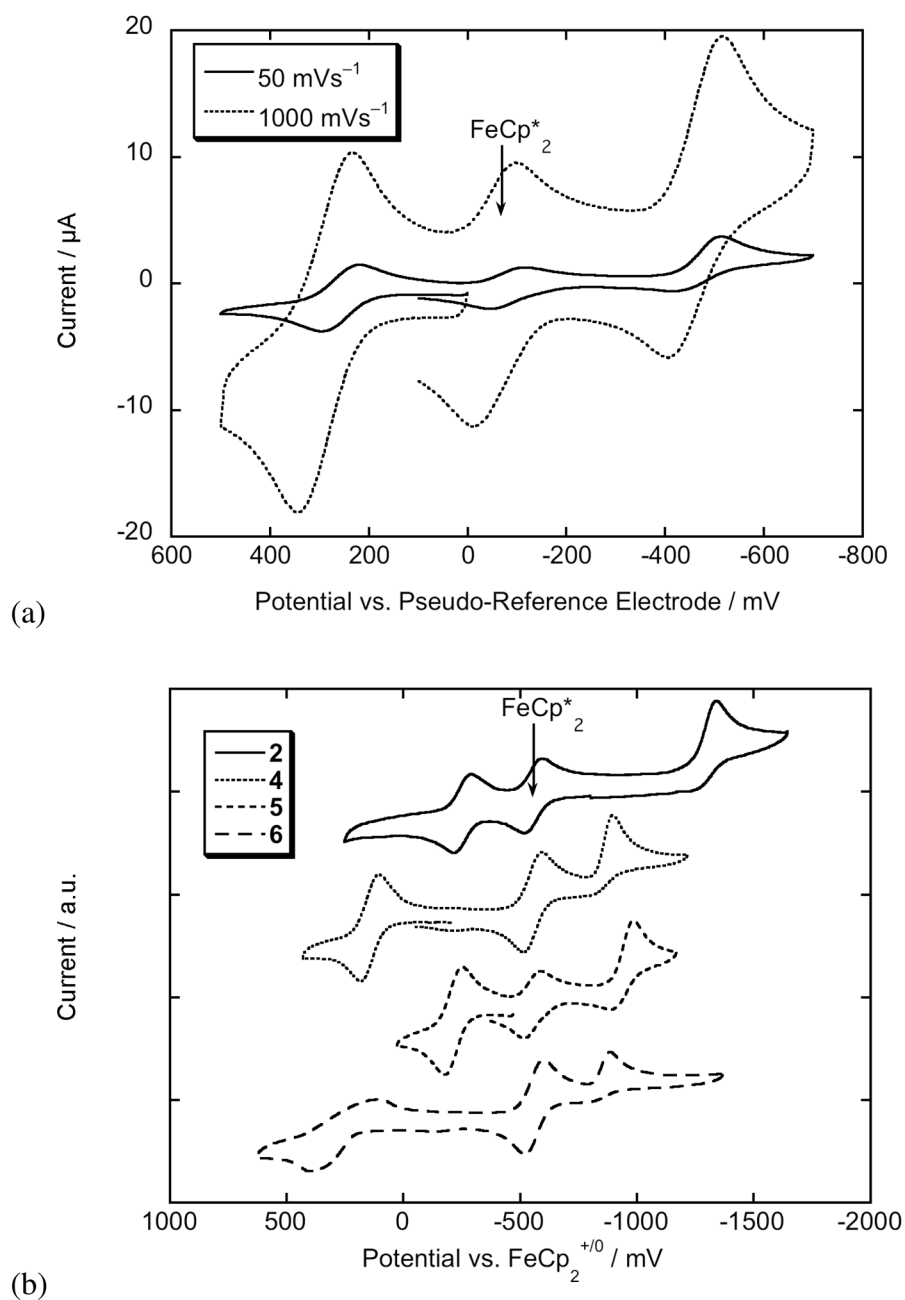


Figure 4. Cyclic voltammograms of metallocene chromophores in $\text{CH}_2\text{Cl}_2/0.1 \text{ M } n\text{Bu}_4\text{NPF}_6$: (a) cyclic voltammogram of **5** at 50 and 1000 mVs^{-1} showing the scan-rate dependence of the reversibility of the $5^{0/-}$ couple; and (b) comparison of cyclic voltammograms (50 mVs^{-1}) of TB vs. SDS derivatives (**2** vs. **5**) and of Fc vs. Fc'' vs. Rc chromophores (**4** vs. **5** vs. **6**). Note that all samples contain FeCp^*_2 ($\text{Cp}^* = \eta^5\text{-C}_5\text{Me}_5$) as an internal standard.

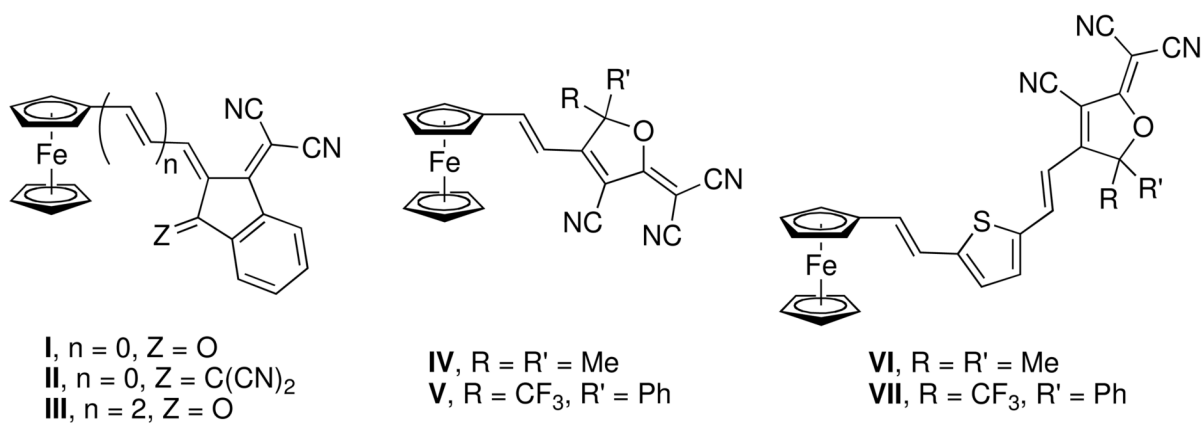


Chart 1.
 Examples of crystallographically characterized ferrocenyl-based chromophores with strong π -acceptor groups.⁹⁻¹¹

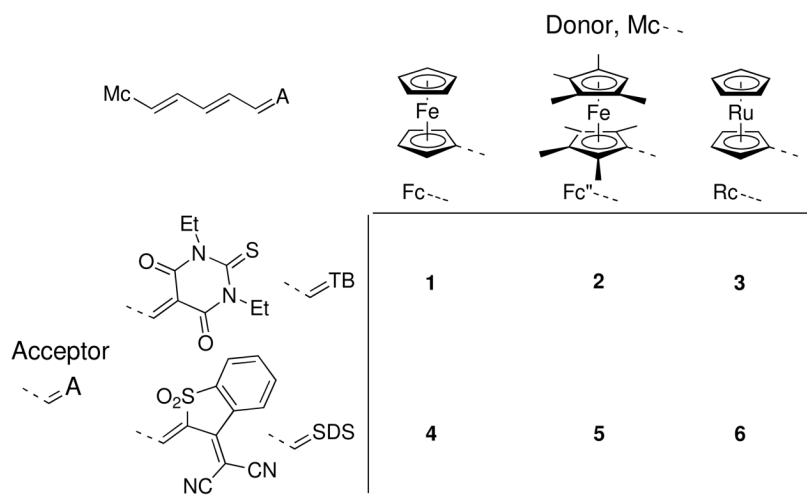


Chart 2.
Compounds for which crystal structures were determined in this work.

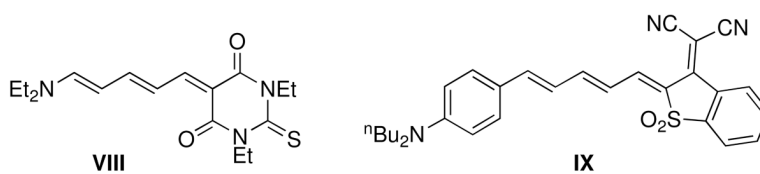


Chart 3.
Organic chromophores discussed in the text.

Table 1

Selected Crystallographically Determined and DFT/B3LYP (in italics) Bond Lengths^a and Bond-Length Alternation Parameters for 1–6.

	1	2A	2B	3	4	5	6
C _M –C _u	1.448(2)	1.440(6)	1.427(7)	1.447(3)	1.444(3)	1.419(5)	1.446(5)
	<i>1.447</i>	<i>1.444</i>		<i>1.446</i>	<i>1.445</i>	<i>1.440</i>	<i>1.444</i>
C _e –C _β	1.354(2)	1.357(6)	1.361(6)	1.353(3)	1.360(3)	1.355(5)	1.349(5)
	<i>1.361</i>	<i>1.366</i>		<i>1.362</i>	<i>1.363</i>	<i>1.369</i>	<i>1.364</i>
C _β –C _γ	1.426(2)	1.437(6)	1.417(6)	1.429(3)	1.425(3)	1.418(5)	1.422(4)
	<i>1.429</i>	<i>1.428</i>		<i>1.429</i>	<i>1.426</i>	<i>1.424</i>	<i>1.426</i>
C _γ –C _δ	1.367(2)	1.369(6)	1.358(6)	1.363(3)	1.363(3)	1.357(5)	1.361(5)
	<i>1.370</i>	<i>1.372</i>		<i>1.371</i>	<i>1.371</i>	<i>1.374</i>	<i>1.372</i>
C _δ –C _ε	1.420(2)	1.433(7)	1.404(7)	1.421(3)	1.409(3)	1.412(5)	1.416(5)
	<i>1.422</i>	<i>1.419</i>		<i>1.421</i>	<i>1.422</i>	<i>1.418</i>	<i>1.421</i>
C _ε –C _A	1.372(2)	1.366(6)	1.357(6)	1.367(3)	1.364(3)	1.372(5)	1.373(5)
	<i>1.377</i>	<i>1.379</i>		<i>1.378</i>	<i>1.373</i>	<i>1.376</i>	<i>1.374</i>
BLA	0.067	0.073	0.057	0.071	0.064	0.054	0.067
	<i>0.063</i>	<i>0.058</i>		<i>0.062</i>	<i>0.062</i>	<i>0.054</i>	<i>0.060</i>
M–C _u	3.106	3.076	3.056	3.194	3.070	3.098	3.162
	<i>3.152</i>	<i>3.150</i>		<i>3.285</i>	<i>3.144</i>	<i>3.149</i>	<i>3.273</i>

^aSee Figure 3 for definitions of bond lengths.

Table 2

^1H - ^1H Coupling Constants (in Hz) for **1-6** and **IX** in CD_2Cl_2 .^a

	1	2	3	4	5	6	IX
$\text{H}_\alpha\text{H}_\beta$	15.1	b	15.1	15.0	14.5	15.0	14.7
$\text{H}_\beta\text{H}_\gamma$	11.5	10.9	11.5	10.9	11.8	10.8	11.2
$\text{H}_\gamma\text{H}_\delta$	14.0	13.5	14.0	b	b	b	13.4
$\text{H}_\delta\text{H}_\epsilon$	12.6	12.8	12.7	11.7	12.7	11.6	12.4

^a H_α - H_ϵ refer to the hydrogen atoms attached to C_α - C_ϵ respectively, as defined in Figure 3.

^b Not determined due to overlap of peaks.

Table 3

Electrochemical Potentials (V vs. FeCp₂⁺⁰) in CH₂Cl₂/0.1 M ⁿBu₄NPF₆ for **1–6** and Related Compounds.

	1	2	3	4	5	6	IX	Fe(C ₃ Me ₄ H) ₂	RuCp ₂
$E_{1/2}^{+0}$	+0.16	-0.25	+0.31 ^a	+0.15	-0.21	+0.41 ^a	+0.37 ^b	-0.45 ^c	+0.56 ^a
$E_{1/2}^{0-}$	-1.21 ^b	-1.34 ^b	-1.24 ^b	-0.89 ^b	-0.96 ^b	-0.88 ^b	-0.93 ^b	-	-

^aIrreversible; values given are peak potentials, E_{ox} , at 50 mVs⁻¹.

^bEC-type processes.

^cData from reference 66.

Table 4

IR C=O and C≡N Stretching Frequencies (KBr, cm^{-1}) for TB and SDS Derivatives, Respectively.

	ν_{CO}			ν_{CN}			
1	2	3	4	5	6	IX	SDS-H₂
1665	1656	1662	2214	2208	2215	2209	2231

Table 5
Sum of Mulliken Charges on Donor, Bridge, and Acceptor Portions of **1-6** and **IX**.

	1	2	3	4	5	6	IX
D	0.090	0.191	0.128	0.126	0.251	0.154	0.335
Bridge	0.159	0.085	0.148	0.204	0.164	0.225	0.085
A	-0.249	-0.276	-0.276	-0.330	-0.415	-0.378	-0.420